HHS Public Access

Author manuscript

Addict Neurosci. Author manuscript; available in PMC 2023 January 12.

Published in final edited form as:

Addict Neurosci. 2022 December ; 4: . doi:10.1016/j.addicn.2022.100047.

Adolescent intermittent ethanol exposure reduces astrocyte-synaptic proximity in the adult medial prefrontal cortex in rats: Reversal by gabapentin

Kati L. Healey[a,1,*], **Amelia Bell**[a,1], **Michael D. Scofield**[b], **H.S. Swartzwelder**[a]

[a]Department of Psychiatry and Behavioral Sciences, Duke University School of Medicine, Durham, N.C. 27710, United States of America

[b]Department of Anesthesia and Perioperative Medicine, Medical University of South Carolina, Charleston, S.C. 29425, United States of America

Abstract

Alcohol consumption in adolescence causes multiple acute negative changes in neural and behavioral function that persist well into adulthood and possibly throughout life. The medial prefrontal cortex (mPFC) and dorsal hippocampus are critical for executive function and memory and are especially vulnerable to adolescent ethanol exposure. We have reported that astrocytes, particularly in the mPFC, change both in morphology and synaptic proximity during adolescence. Moreover, adolescent intermittent ethanol (AIE) exposure produces enduring effects on both astrocyte function and synaptic proximity in the adult hippocampal formation, and the latter effect was reversed by the clinically used agent gabapentin (Neurontin), an anticonvulsant and analgesic that is an inhibitor of the VGCC $\alpha 2\delta 1$ subunit. These findings underscore the importance of investigating AIE effects on astrocytes in the mPFC, a region that undergoes marked changes in structure and connectivity during adolescence. Using astrocyte-specific viral labeling and immunohistochemistry, mPFC astrocytic morphology and colocalization with AMPA-(α-amino-3-hydroxy-5-methyl-4-isoxazolepropionic acid) glutamate receptor 1 (GluA1), an AMPA receptor subunit and established neuronal marker of excitatory synapses, were assessed to quantify the proximity of astrocyte processes with glutamatergic synaptic puncta. AIE exposure significantly reduced astrocyte-synaptic proximity in adulthood, an effect that was reversed by sub-chronic gabapentin treatment in adulthood. There was no effect of AIE on astrocytic glutamate homeostasis machinery or neuronal synaptic proteins in the mPFC. These findings indicate a possible glial-neuronal mechanism underlying the effects of AIE on frontal lobe-mediated behaviors and suggest a specific therapeutic approach for the amelioration of those effects.

[*]Corresponding author. kati.healey@duke.edu (K.L. Healey).
[1]These authors have contributed equally to this work.

Declaration of Competing Interest

The authors declare that they have no known competing financial interests or personal relationships that could have appeared to influence the work reported in this paper.

Supplementary materials

Supplementary material associated with this article can be found, in the online version, at doi:10.1016/j.addicn.2022.100047.

Keywords

Alcohol; Adolescent; Astrocyte; Synaptic; Medial prefrontal cortex

Introduction

Alcohol consumption during adolescence, approximately age 12-18, is a significant public health concern and causes multiple behavioral and neural deficits that persist well into adulthood [16]. Adolescence is critical for cognitive, social, and neurological development and is a period during which the brain is vulnerable to various insults, including alcohol exposure. Alcohol use is often initiated in adolescence and is used in distinct binge patterns and at high doses [10]. Binge patterns of alcohol use in adolescence lead to negative consequences such as elevated risk of addiction, deficits in memory, and social consequences [26,46]. In addition, there are persistent long-term consequences such as criminal convictions, homelessness, and cognitive deficits such as poorer verbal and visuo-spatial memory and elevated perseveration [16,27,28,59]. Further, altered developmental trajectories of temporal and frontal lobe structures have been shown across adolescence and early adulthood in heavy drinking individuals [48]. These reported deficits indicate persistent adolescent alcohol-induced alterations to brain regions such as the hippocampus and prefrontal cortex, two interconnected regions that are integral for executive function and memory [37]. Adolescence can be modeled in rodent studies, where postnatal day (PND) 28-55 correspond with human adolescence 12-18 years [45]. Animal models of adolescent binge alcohol consumption (adolescent intermittent ethanol, AIE) show similar deficits in prefrontal cortical (PFC) and hippocampal structure and function (for review see [9,47]). However, little is known about the cellular mechanisms that underlie these persistent alcohol-induced deficits.

Recently, it has become apparent that AIE-induced alterations are not just neuronal but also glial. Adult dorsal hippocampal astrocytes, in animals with a history of AIE, exhibited reduced proximity with excitatory glutamatergic synapses, but no change in astrocyte morphology [20], and elevated expression of astrocytic glutamatergic homeostatic machinery [19]. Of note, we previously reported no differences in hippocampal astrocyte surface area, volume, or synaptic proximity between pre-adolescence (PND 24), early-adolescence (PND 30), late-adolescence (PND 44-47) or adulthood (PND 70) [53]. In adulthood, after exposure to AIE, expression of voltage-gated calcium channel (VGCC) subunit $\alpha 2\delta 1$ was upregulated in the dorsal hippocampus as was their endogenous ligands, astrocyte-released thrombospondins (TSP) [39]. This suggests that, while AIE may reduce synaptogenesis during adolescence, the long-term consequence of AIE appears to be an aberrant increase in excitatory synaptogenesis, which may account for maladaptive augmentation of glutamatergic (NMDA receptor-mediated) neurotransmission [51] and synaptic plasticity [38] in adulthood after AIE. Further, AIE caused a significant increase in astrocyte reactivity in adulthood as reflected in enhanced GFAP expression in hippocampal area CA1 [39]. Additionally, this could reflect an increased number of astrocytes as astrocyte morphology in this region is unchanged by AIE [20].

Although much of the extant literature examining the link between AIE and astrocytes has been conducted in the hippocampal formation, the aim of this study is to investigate the ways which AIE may alter astrocyte morphology and synaptic proximity in the medial PFC (mPFC). Both the mPFC and dorsal hippocampus, and coordinated activity within these regions, are critical for executive function and memory, neural functions which have been shown to be affected by adolescent alcohol use [5,11,15]. Comparison of AIE-induced effects on astrocytes in the hippocampus and mPFC could facilitate an understanding of how these distinct, but functionally related, structures respond in parallel to repeated ethanol exposure. Our laboratory has previously shown that mPFC astrocytes increase in volume, surface area, and synaptic colocalization during adolescent development, whereas hippocampal astrocytes do not [53]. This suggests that astrocytes in the mPFC may be more vulnerable to enduring AIE-induced alterations than are hippocampal astrocytes, underscoring the importance of assessing AIE effects on astrocyte-neuronal interactions in the mPFC. Previous studies have shown AIE induces glial alterations in the adult PFC as it decreases overall glial number [23], elevates the microglia marker CD11b and primes PFC microglia responsivity to stress [60], further implicating the mPFC as a region of interest for persistent AIE effects.

AIE causes decreased physical proximity between astrocytes and synapses in area CA1 of the dorsal hippocampus, an effect which persists into adulthood [20] and was reversed by treatment with gabapentin (Neurontin) [20]. Notably, gabapentin treatment which reversed these AIE-induced astrocyte deficits was given in adulthood, long after the exposure to ethanol had ceased. Gabapentin is an anti-convulsant and analgesic drug that is also used as an adjunct treatment in certain affective disorders. It interacts with the astrocytic glutamate transporter, GLT-1, $\alpha 2\delta 1$ subunits of voltage-gated Ca^{2+}channels, and presynaptic $GABA_B$ receptors [12,30,49,52]. All of these targets have been found to be altered by AIE in the hippocampus by our laboratory [7,19,39],including an AIE elevation of thrombospondins (TSPs), which gabapentin is an inhibitor of the VGCC $\alpha 2\delta 1$ subunit which is activated by TSPs [12,30].

These hippocampal findings, along with the connectivity between the dorsal hippocampus and mPFC and the marked changes of the mPFC during adolescence, underscore the importance of investigating effects of AIE on astrocytes in the mPFC. We hypothesize that AIE will cause a decrease in colocalization of astrocyte and glutamatergic synaptic markers (AMPA-receptor mediated) in the mPFC and that this effect will be reversed by gabapentin. We also predict that AIE may affect astrocyte morphology, and lock-in the adolescent phenotype of smaller astrocytes [47,53]. We also investigated the effect of AIE on adult mPFC expression of astrocytic glutamatergic homeostasis machinery and neuronal synaptic proteins. The results from this experiment will have important mechanistic and clinical implications to understand and combat the persistent effects of adolescent alcohol use.

Methods

The following techniques used in this experiment were conducted in accordance with the guidelines of the American Association for the Accreditation of Laboratory Animal Care

and the National Research Council's Guide for Care and Use of Laboratory Animals and were approved by the Duke University Institutional Animal Care and Use Committee. All imaging and analyses were performed by investigators blind to the treatment groups of the animals or tissue samples.

Experiment 1

Animals, ethanol exposure, and gabapentin injections—Twenty-eight adolescent male Sprague Dawley rats (Charles River, Raleigh, NC, USA) were received on postnatal day (PND) 25. Animals were pair housed with *ad libitum* access to water and food (5001 Rodent Diet; LabDiet, St. Louis, MO, USA). They were given five days to habituate to the vivarium on a reversed 12-hour light: 12-hour dark cycle. Intermittent dosing by intragastric gavage (i.g.) with either ethanol (5 g/kg, 35% EtOH; Decon Labs, Prussia, PA, USA) or isovolumetric water (AIW) was administered during adolescence (PND 30-45) [50]. Animals were given a total of 10 doses over 16 days on a 2-day on, 1-day off, 2-day on, 2-day off schedule. This ethanol dosage was chosen to produce blood ethanol concentrations (BECs) similar to those of humans during an episode of "binge drinking", defined as five or more drinks for males or four or more drinks for females [24,61]. It was previously found that male rats of the same age and strain as those used in this study that received 5 g/kg ethanol (i.g., 35% EtOH) achieved mean BEC of 199.7 mg/dl (± 19.9) 60 minutes after the first ethanol dose and 172.8 (± 13.3) 60 minutes after the last ethanol dose [38]. This is consistent with human adolescent BECs during binge drinking episodes [24]. To ensure proper intoxication levels, BECs and intoxication scores were routinely assessed. However, blood for BEC analysis was acquired from sentinel animals dosed concurrently but excluded from experimental procedures to avoid the stress of blood sampling as a confounding factor. Surgeries were performed approximately one week after the last water or ethanol dose (see below). Two weeks after surgeries, animals were treated for 5 consecutive days with either gabapentin (100 mg/kg in sterile 0.9% NaCl intraperitoneal, (i.p.); Chem-Impex International, Inc., Wood Dale, IL, USA) or its vehicle, isovolumetric saline. AIW = Adolescent Intermittent Water (i.g), AIE = Adolescent Intermittent Ethanol (5 g/kg, i.g.), VEH = vehicle (0.9% sterile saline, i.p.), GBP = gabapentin (100 mg/kg, i.p.). Animals were divided into four treatment groups: AIW+VEH (n = 4), AIE (n = 5), AIW + GBP n = 5), AIE + GBP (n = 4). Seven animals were removed due to injection outside of target region or lack of viral transfection, and three animals were removed because astrocyte images did not meet minimum threshold of florescence. Three days after the final gabapentin or vehicle treatment, all animals underwent cardiac perfusion with 4% paraformaldehyde (Fig. 1A).

Viral surgery—One week after the final water or ethanol dose, stereotaxic surgery was performed on all animals for viral injection into the left medial prefrontal cortex (+3.3 mm anterior/posterior; −0.6 mm medial/lateral; −3.5 mm dorsal/ventral) [31]. Animals were anaesthetized with ketamine (90 mg/kg, i.p.; Fort Dodge Animal Health, Fort Dodge, IA, USA) and xylazine (7 mg/kg, i.p.; Akron, Lake Forest, IL, USA), given meloxicam (2 mg/kg, subcutaneous, Putney, Fort Worth, TX, USA) as an analgesic, and secured in the stereotaxic instrument. 1μL of rAAV5/GFAP-LCK-GFP (LCK-GFP) (~1×10^{12} viral particles/ml; UNC Vector Core, Chapel Hill, NC, USA) was infused at a rate of 0.1 μL/minute, using a 33-gauge injector needle, followed by 15 minutes of diffusion time

[20,41,42,54]. This virus has an associated green fluorescent protein (GFP) and lymphocyte protein tyrosine kinase (LCK) tag. LCK is a tyrosine kinase which aids in the insertion of the GFP into the membrane for astrocyte visualization.

Immunohistochemistry—Immediately after cardiac perfusion, brains were harvested and post-fixed in 4% paraformaldehyde for two hours and then transferred to a 30% sucrose phosphate-buffered saline (PBS) solution. 100-μm coronal slices containing the mPFC were collected and then blocked with 2% NGS and 2% Triton-X 100 in 0.1 M PBS (PBST) for 90 minutes. Sections were then incubated in primary antibodies (Chicken anti-GFP, 1:1000, Abcam, Cambridge, MA, USA, Cat#Ab13970; anti-AMPA receptor 1, 1:500, Cell signaling Technology, Danvers, MA, USA, Cat#13185) diluted in PBST with shaking overnight at 4 °C. Sections were then washed three times, for five minutes each, in PBST. This was followed by secondary incubation performed at 4 °C with species-appropriate secondary antibodies (goat anti-chicken, Alexa-Flour 488, 1:2000; goat anti-rabbit, Alexa-Flour 568, 1:2000; Life Technologies, Carlsbad, CA, USA, Cat# ab150169) overnight in PBST. Again, after incubation, slices were washed three times, five minutes each, in PBST prior to being mounted on slides with Pro Long Gold Antifade (Life Technologies, Carlsbad, CA, USA). Immunohistochemistry protocols have been established and optimized by the Scofield laboratory and ours [41,53].

Imaging—Individual astrocytes unimpacted by competing signal from neighboring labeled cells within the region of interest (medial prefrontal cortex, mPFC) were imaged. An average of four astrocytes per animal was acquired from either the prelimbic or infralimbic medial prefrontal cortex (Paxinos & Watson (1997) (Fig. 1B). The mPFC includes the infralimbic and prelimbic regions, and astrocytes exhibited no significant morphometric differences between the subregions, as determined by a two-tailed Student's t-test with alpha set at $p < 0.05$. In addition, synaptic puncta marked by immunofluorescent GluA1 were imaged for astrocyte-synaptic proximity analyses. Acquisition of images was performed on a Leica DMi8, laser scanning, confocal microscope equipped with HyD detectors and a 100x objective (NA 1.3, Wetzlar, Germany). Images were acquired by bidirectional scanning with a X phase shift of 30 and a pinhole of 1 Airy unit. Images were acquired at a resolution of 2048×2048 and a z-step size of 0.10 μm. These settings produced images with X and Y dimensions of 116.5 μm x 116.5 μm. Confocal data sets were deconvolved using Huygens Professional software (Scientific Volume Imaging, VB Hilversum, Netherlands). Finally, all deconvolved data were imported into Imaris software (Bitplane, Zurich, Switzerland), and an experimenter, blinded to treatment groups, isolated the boundary of individual astrocytes using the surface function to generate a three-dimensional region of interest (ROI) reflecting the dimensions of the imaged astrocyte. Astrocyte volume and surface area were calculated from this ROI. In order to control for the possibility that regions of the astrocyte were not captured, morphological data were analyzed as the ratio of surface area to volume of the ROI to generate a normalized index of astrocyte morphology [8]. The spot detection algorithm of the Imaris software was used to digitally identify and mark GluA1 puncta. The density of synaptic puncta in the image was measured as the ratio of the total number of spots to the volume (μm^3) of the image to compare overall synaptic density between treatment groups. Finally, astrocyte-synaptic contact was estimated by measuring co-registration of the

rendered astrocyte surface with the synaptic puncta (GluA1). The spot detection algorithm was used again to identify synaptic puncta for which the center of puncta contacted the astrocytic rendered surface [2,21,40]. Astrocyte-synaptic proximity was expressed as the ratio of the number of GluA1 spots normalized to the volume of the corresponding astrocyte ROI (μm^3).

Experiment 2

Animals and ethanol dosing—Sprague Dawley dams with pups (Charles River, Raleigh, NC, USA) were received with pups PND 14 and allowed to habituate for 1 week. Pups were weaned on PND 21 and pair housed with *ad libitum* access to water and food. They were given seven days to habituate to colony room with conditions identical to Experiment 1. Intermittent i.g. dosing with either ethanol (5g/kg, 35% EtOH) or isovolumetric water (AIW) was administered during adolescence (PND 28-50) [50]. Animals were given a total of 14 doses over 22 days on a 2-day on, 1-day off, 2-day on, 2-day off schedule. After dosing, animals aged into adulthood and, at PND 80, were sacrificed by rapid decapitation and brains harvested for medial prefrontal cortex (infralimbic and prelimbic regions). These methods differ from *Experiment 1* because they are new standards set by the NADIA consortium to reduce the stress of animal delivery and to optimize AIE procedures to include all of adolescence. We do not expect the additional AIE doses to effect outcome as the NADIA has found several different AIE exposure periods to produce robust effects [9].

Tissue preparation—Following previously reported methods [19], mPFC tissue was Dounce homogenized by hand in a sucrose-HEPES buffer [320 mM sucrose, 10 mM HEPES, 1 mM Na Fluoride, 1 mM Na Orthovanadate activated, 1:100 Protease Inhibitors ("Complete" PI tablets, cat# 04693159001, Roche, Sigma-Aldrich, St. Louis, MO)]. Samples were spun at 23,000 x *g* and 4 °C for 30 minutes, and the supernatant was removed. The resulting pellet was resuspended in 250 μl of lysis buffer (50 mM Tris-HCL, 1 mM EGTA, 1 mM EDTA, 1 mM Na Fluoride, 1 mM Na Orthovanadate activated, 1:100 protease inhibitors, 0.5% Triton X-100) and rotated for 15 minutes at 4 °C. Next, samples were centrifuged at 12,000 x *g* and 4 °C for 20 minutes, and the supernatant (Triton-soluble extra-synaptic fraction) was collected. Finally, the remaining pellet (Triton-insoluble synaptic fraction) was resuspended in 100 μl of 2% LDS and sonicated.

Immunoblot analysis—Protein concentrations were determined using the Pierce BCA Protein Assay Kit (cat#23225, ThermoFisher Scientific, Waltham, MA). Four animals did not have sufficient protein concentration to be included in the synaptic fraction immunoblot analyses and were removed from those analyses (AIW n=2, AIE n=2). 8 μg of protein was resolved by SDS-PAGE (12% Tris-HCL gels, cat# 4561045, Bio-Rad, Hercules, CA) and transferred to polyvinylidene fluoride membrane (cat#IPFL00010, Sigma-Aldrich). Membranes were then stained with REVERT 700 Total Protein Stain (cat#926-11011, LI-COR, Lincoln, NE), imaged in Odyssey FC (700 nm, LI-COR), and blocked in Intercept blocking buffer (cat#927-60003, LI-COR) for one hour at room temperature. Membranes were next probed with primary antibodies overnight at 4 °C [Guinea Pig anti-GLT1, 1:5000 (cat#AB1783, Millipore Sigma, St, Louis, MO) and Rabbit anti-EAAT1, 1:3000 (cat#ab416,

Abcam, Cambridge, MA)] and followed the next day with IRDye secondary antibodies diluted to 1:15,000 [800CW Donkey anti-Guinea Pig (cat#926-32411, LI-COR) and 680RD Donkey anti-Rabbit (cat#926-68073, LI-COR)] for 90 minutes at room temperature. Blots were imaged using Odyssey Fc (700 and 800 nm, LI-COR). Membranes were then stripped using NewBlot IR Stripping Buffer (cat#928-400028, LI-COR), blocked again using blocking buffer, and probed with different primary antibodies [Mouse anti-CACNA2D1, 1:1000 (cat#MA3921, Invitrogen, Grand Island, NY) and Rabbit anti-PSD95, 1:1000 (cat#ab18258, Abcam)]. This was followed with IRDye secondary antibodies diluted to 1:15,000 [800CW Donkey anti-Mouse (cat#926-32210, LI-COR) and 680RD Donkey anti-Rabbit] and again imaged using Odyssey Fc. Optical densities of all bands and total protein stain were quantified using Image Studio software (LI-COR) and adjusted to background subtraction using the standard LI-COR Image Studio-defined parameters. Bands of interest (one lane per independent brain sample) were normalized to REVERT Total Protein Stain using the lane normalization factor (LNF) recommended by LI-COR (Signal/LNF).

Data analysis.

Experiment 1.—Data for all immunohistochemistry dependent measures were averaged for each animal and analyzed by animal using the two-way analysis for variance (ANOVA) functions in Prism (San Diego, CA, USA). Significant interaction effects were followed by post-hoc analyses of simple main effects based on a-priori hypotheses, planned comparisons, using Fisher's least significant differences tests. Alpha was set at $p < 0.05$ for all main effect analyses. However, due to the low power of interactions at a given sample size relative to main effects, interactions at $p < 0.1$ were examined as to whether lower-order effects were detectable after subdivision of the interactive variables [44]. This criterion for interactions was used to identify interactive factors requiring subdivision for lower-order tests of effects of AIE and gabapentin [1,4,6,17,36]. There is no widespread agreement in the field on controlling for the False Discovery Rate when making planned comparisons or its effects on Type I error. *Experiment 2:* Data for all dependent measures were assessed by two-tailed Student's t statistic with alpha set at $p < 0.05$.

Results

Astrocyte morphology

After the experimental timeline outlined in Fig. 1A, the LCK-GFP infusions in the mPFC produced strong labeling of cortical astrocytes (Fig. 1C) which allowed for analysis of 73 astrocytes across the infralimbic and prelimbic regions of the mPFC (Fig. 1B). The surface area and volume of the analyzed astrocytes as well as the ratio of these measures were not significantly different between the infralimbic and prelimbic subregions (Data not shown: $t(71) = 0.70$, $p > 0.05$, $t(71) = 0.28$, $p > 0.05$, $t(71) = 1.28$, $p > 0.05$, respectively), allowing for analysis of both subregions together. Astrocyte morphology was expressed as the ratio of surface area to volume (SA:V). As determined by a simple main effect, AIE exposure resulted in a significant reduction in the ratio of SA:V ($F_{(1,14)} = 4.87$, $p = 0.04$, Fig. 1D). However, AIE exposure had no effect on surface area or volume individually (Data not shown: $F_{(1,14)} = 0.30$, $p > 0.05$, $F_{(1,14)} = 1.56$, $p > 0.05$, respectively). Moreover, gabapentin treatment had no effect on the ratio of SA:V ($F_{(1,14)} = 1.07$, $p > 0.05$, Fig. 1D), indicating

there was no significant alteration of astrocyte morphology by gabapentin alone. Finally, there was no interaction of AIE and gabapentin on SA:V ($F_{(1,14)} = 0.01$, $p > 0.05$, Fig. 1D).

Density of synaptic punta

Staining for GluA1 as a marker for synaptic puncta resulted in a strong punctate labeling throughout the tissue, which was consistent between animals (Fig. 1C). The density of GluA1 synaptic puncta was not significantly different between the infralimbic and prelimbic subregions allowing for analysis of both subregions together (Data not shown: $t(71) = 0.27$, $p > 0.05$). To confirm that any effect of treatment group on astrocyte-synaptic proximity was not confounded by an overall significant difference in the number of synapses in tissue samples, the total density of synapses (GluA1 puncta/image volume) was evaluated and compared between groups. As expected, there was no effect of either AIE exposure ($F_{(1,14)}$) = 0.16, $p > 0.05$,), gabapentin ($F_{(1,14)} = 0.32$, $p > 0.05$,), or their interaction ($F_{(1,14)}$) = 0.30, $p > 0.05$,) on the overall density of synaptic puncta (Fig. 2B).

Astrocyte-synaptic proximity

Consistent with previous findings in the hippocampal formation [20], and with the hypotheses that drives this study, AIE exposure and gabapentin treatment during adulthood differentially affected proximity of perisynaptic astrocytic processes to glutamatergic synapses. There was an interaction between AIE and gabapentin on astrocyte-synapse proximity (astrocyte-synaptic contact/astrocyte volume; $F_{(1,14)} = 3.57$, p = 0.08, Fig. 2A,C) that prompted follow-up tests of the effects of AIE and gabapentin. Post-hoc analyses revealed that AIE treated animals had significantly reduced astrocyte-synaptic proximity compared to AIW treated control animals (p = 0.03). This effect was reversed by treatment with gabapentin in adulthood. Specifically, astrocytes from animals treated with AIE + gabapentin had significantly increased astrocyte-synaptic proximity compared to animals treated with AIE alone (p = 0.02). Additionally, astrocyte-synaptic proximity was not significantly different between animals treated with AIE + gabapentin compared to those treated with AIW alone or AIW + gabapentin ($p > 0.05$).

Western blots

Prelimbic and infralimbic prefrontal cortical (mPFC) tissue was harvested and separated into synaptic (PSD-95 enriched) and extra-synaptic sub fractions for assessment of protein levels of astrocytic [glutamate transporter-1 (GLT-1), excitatory amino acid transporter 1/ Glutamate Aspartate Transporter 1 (GLAST)] and neuronal markers [voltage-gated calcium channel subunit $\alpha 2$-$\delta 1$, post-synaptic density marker 95 (PSD-95)]. We found no effect of AIE on synaptic mPFC protein expression of GLT-1, GLAST, $\alpha 2$-$\delta 1$ or PSD-95 ($p>0.05$, Fig. 3A, Supplemental Table 1, Supplemental Fig. 1). Similarly, there was no effect of AIE on GLT-1, GLAST, $\alpha 2$-$\delta 1$ or PSD-95 extra-synaptic mPFC protein expression (Fig. 3B, Supplemental Table 1, Supplemental Fig. 2). Student's t statistics are presented in Supplemental Table 1.

Discussion

The principal findings of this study were the reduction of mPFC astrocyte-synaptic proximity in adulthood after AIE exposure and the reversal of that effect by gabapentin treatment in adulthood. Specifically, we observed a reduction in colocalization of synaptic puncta and astrocyte membrane per unit volume of astrocyte in animals exposed to AIE compared to water controls. It is likely that this deficit was due to a reduction in astrocyte-synaptic proximity rather than a global reduction in the number of synapses because there was no AIE-induced change in the overall density of GluA1 synapses within the region of interest, nor in the expression of synaptic PSD-95 protein in mPFC tissue generally. Importantly, the AIE effect was present in adulthood long after the termination of ethanol exposure, indicating that the effects of AIE on mPFC astrocyte-neuronal proximity persist into adulthood, as might their behavioral consequences, underscoring the public health relevance of these findings.

Astrocytes exhibit a unique morphology, and differences in astrocyte morphometrics have been associated with distinct aspects of astrocyte function [29]. We have reported previously that mPFC astrocytes are larger, by surface area and volume, in adulthood compared to adolescence [53]. Our current finding that adult animals treated with AIE exhibit smaller astrocytes than controls, could indicate a lock-in of this adolescent phenotype, comparable to other observations of the persistence of adolescent neural and behavioral characteristics into adulthood after AIE (see [9,47] for review). Smaller astrocytes can be detrimental in the adult brain because adult astrocytic size is closely associated with astrocyte function and with several affective and substance abuse disorders [22]. Smaller astrocytes have less ensheathment of synapses as well as reduced expression of important astrocytic proteins such as glial-fibrillary acid protein (GFAP) and aquaporin receptors (AQP4) [32]. Additionally, morphological changes cause deficits in astrocyte functioning such as reduced tone of signaling molecules and trophic factors, dysregulation of glutamate metabolism and homeostasis, and reduced astrocyte connectivity [32]. Thus, an AIE-induced lock-in of adolescent astrocyte morphology could markedly alter adult astrocyte function, particularly astrocyte-synaptic interaction. Moreover, changes in astrocyte structure have been linked to the effects of several abused drugs [19,41,43,54] as well as other neuropsychiatric disorders such as frontotemporal dementia [58] and major depressive disorder [35]. Thus, the AIE-induced reduction of the ratio of astrocyte surface area to volume in adulthood, which we report here, could indicate a mechanism underlying previously reported changes in prefrontal-mediated behaviors after AIE.

The AIE-induced reduction in mPFC astrocyte-synapse proximity in adulthood is consistent with both our apriori hypothesis and with previous findings in the dorsal hippocampus [20]. As noted, this is likely a true reduction in astrocyte-synaptic proximity and not a change in synaptic number, as there was no effect of AIE on overall numbers of GluA1 puncta or on PSD-95 protein expression. Supporting this, it has been shown that AIE has no effect on glutamatergic proteins in the prelimbic cortex (PrL), however there was an increase in the density of immature dendritic spines [56]. This is not inconsistent with our findings, as immature spines (long thin) have less GluA1 than mature spines [18], but it does indicate an area that needs to be investigated further. Moreover, the observed reduction of astrocyte-

synaptic proximity is consistent with growing evidence of similar reductions in multiple brain regions after exposure to drugs of abuse. For example, it has been found that astrocyte-synaptic proximity was reduced in the nucleus accum bens core after self-administration of methamphetamine [43] and cocaine [41,54] and our own findings of AIE-induced reduction in the hippocampus [20]. However, these effects are not consistent across brain regions, as cocaine self-administration was found to have no effect on astrocyte-synaptic proximity in the PrL and basolateral amygdala [54]. Finally, it is worth emphasizing that the present effect was observed in adulthood long after the termination of ethanol exposure, indicating that AIE induces persistent alterations on mPFC astrocyte-neuronal proximity, long after ethanol exposure has ceased. As previously noted, many behaviors modulated by the PFC are altered by adolescent ethanol exposure, including executive functioning and decision making such as the evaluation of outcomes and motivations [37], as well as some types of risk taking behaviors [34]. The reduction in astrocyte-synaptic proximity in the mPFC and resulting dysregulation of mPFC function, may have behavioral consequences that are risk factors for developing or sustaining alcohol use disorders, underscoring the public health relevance of these findings.

One limitation of the present study is that it used tissue from male animals only. Thus, the findings must be interpreted cautiously, particularly with respect to their generalizability. Although there have not been extensive studies of the possible sex-mediated effects of AIE on the mPFC, per-se, there are some indications that AIE may affect PFC-mediated function differentially in males and females. One behavioral domain that is linked strongly to PFC function, and is also affected by ethanol, is behavioral flexibility. AIE affects behavioral flexibility in both sexes, but there are some sex-differences. For example, [3] found that AIE promoted a habit-like strategy in an operant task (considered behavioral inflexibility) in female, but not male, rats; and Varlinskaya et al. [57] reported AIE-induced deficits in behavioral flexibility on a set-shifting task in male rats but not in females. In contrast, although AIE was shown to produce a habitual behavioral strategy (i.e. behavioral inflexibility) in an instrumental sensory-specific satiation procedure, that effect was observed in both sexes [55]. Similarly, on an operant learning task [13] observed AIE-induced behavioral flexibility that was not sex-dependent; and Macht et al. [25] observed AIE-induced deficits in behavioral flexibility on a battery of spatial and non-spatial learning tasks that were not sex-dependent. Although equivocal with respect to the interaction of AIE and sex on PFC-mediated function, these studies underscore the need for future studies of this type to include sex as an independent variable.

In addition, although sex differences in astrocyte morphology in the mPFC have not thoroughly studied, there do appear to be sex differences in astrocyte density and morphology in some brain regions. For example, male mice have greater astrocyte density and complexity in the amygdala than females [33]. In contrast, astrocytic complexity in the hippocampal formation is greater in females than in males [14]. These sex differences in astrocyte density and morphology suggest that the present results in male mPFC must be expanded to include females in order to extend their translational value and clinical implications.

The reversal of this AIE effect on astrocyte-synaptic proximity by gabapentin is significant for two reasons. First, gabapentin treatment was very brief, consisting of only five doses, and did not affect astrocyte-synaptic proximity in control animals (i.e. those not exposed to AIE). This is consistent with the safety profile of gabapentin (Neurontin) as it is used clinically. The fact that gabapentin given in adulthood reversed this enduring effect of alcohol exposure during adolescence further supports the translational relevance of this finding, as it suggests that an ameliorative treatment could be given outside of the developmental window of adolescence. Finally, the common clinical use of gabapentin contributes to the translational significance of this project. Although the use of gabapentin, or other agents with similar mechanisms, as a treatment to alleviate AIE effects in a clinical setting is not immediately justified by the present findings, its efficacy in this animal model indicates it is a promising avenue for future clinical research.

The mechanism whereby gabapentin ameliorated the effect of AIE on astrocyte-neuronal proximity in this study is unclear, though there are several possibilities. The present observed reversal of mPFC AIE effects is consistent with our previous report of gabapentin reversal of AIE-induced astrocyte-neuronal proximity effects in the hippocampal formation [20]. In addition, it is consistent with previous studies from our laboratory in which gabapentin reversed the effects of AIE on NMDA receptor-mediated synaptic currents in hippocampal CA1 pyramidal cells [51]. It is possible that the AIE-induced de-coupling of astrocytes and neurons in the mPFC that we observe here reflects a compensatory thrombospondin-induced increase in excitatory synaptogenesis that leads to an increased NMDA current amplitude like that have observed previously [51]. If so, gabapentin may have ameliorated that effect due to its known ability to antagonize the excitatory synaptogenic effect of thrombospondins at their neuronal $\alpha 2$-$\delta 1$ receptor [12] and thereby reversed the astrocyte-neuronal decoupling action of AIE. Future studies will address that specific mechanism.

Both principal findings regarding astrocyte-synaptic proximity of this study support our original hypotheses which were based on similar findings in the hippocampus. These results support the conclusion that ethanol reduces astrocyte-synaptic proximity in the brain and suggest that other brain regions outside of the frontotemporal system could be similarly affected by AIE. Although these findings suggest that AIE-induced changes that we have observed in hippocampal astrocytes, such as adaptations in expression of astrocytic GFAP, GLT-1, , TSP and neuronal $\alpha 2$D-1 expression [19,39], could also occur in the mPFC after AIE, we found no changes in GLT-1, GLAST, or $\alpha 2$d-1 expression in the present study. This suggests that enduring effects of AIE on mPFC astrocytes may not involve glutamatergic transport through those specific transporters or an alteration of TSP-$\alpha 2$d-1 interaction. However, these findings must be interpreted cautiously because the measures were made using protein expression assays in whole mPFC tissue rather than immunohistochemically in specific regions of interest within the mPFC. Still, they do suggest that other mechanisms might be more likely. For example, we have shown elevated expression of the cystine/glutamate antiporter, xCT, in the adult ventral hippocampus after AIE suggesting that cystine-related mechanisms should be explored in the mPFC. Another interesting hippocampal AIE effect that could be investigated in the mPFC is the upregulation of TSPs during adulthood. As noted above, TSPs are proteins secreted

by astrocytes which act on dendritic spines, through the α2d1 receptor, to promote synaptogenesis [12]. Although α2d-1 expression was not altered in whole mPFC tissue in this study, if TSP expression were altered it would suggest a shift in the dynamic of TSP-α2d1 interaction as a possible mechanism underlying AIE effects on mPFC and associated behavioral functions.

In summary, this study identified one way in which adolescent intermittent ethanol exposure effects the mPFC astrocyte-neuronal relationship: the reduction of astrocyte-synaptic proximity. This is significant because it points toward a specific glial-neuronal mechanism that may underlie some of the effects of AIE on frontal lobe-mediated behavior. Brief systemic gabapentin treatment in adulthood reversed this effect of AIE, pointing to a specific receptor-level mechanism that may mediate AIE effects on neural circuits, and providing a possible therapeutic target for the development of ameliorative treatments for the enduring sequelae of adolescent ethanol exposure.

Supplementary Material

Refer to Web version on PubMed Central for supplementary material.

Funding

This work was supported by National Institute of Health [NADIA grant 3U01AA019925, 2019]

Data Availability

Data will be made available on request.

Abbreviations:

AIE	adolescent intermittent ethanol
AIW	adolescent intermittent water
PAP	perisynaptic astrocyte process
GBP	gabapentin
GluA1	glutamate receptor 1
GLAST	glutamate aspartate transporter 1
PSD-95	post-synaptic density marker
xCT	cystine/glutamate antiporter
GFAP	glial-fibrillary acid protein
AQP4	aquaporin receptors
GFP	green fluorescent protein
LCK	lymphocyte protein tyrosine kinase

VGCC	voltage-gated calcium channel
TSP	thrombospondins

References

[1]. Adigun AA, Wrench N, Levin ED, Seidler FJ, Slotkin TA, Neonatal parathion exposure and interactions with a high-fat diet in adulthood: Adenylyl cyclase-mediated cell signaling in heart, liver and cerebellum, Brain Res. Bull 81 (6) (2010) 605–612, doi:10.1016/j.brainresbull.2010.01.003. [PubMed: 20074626]

[2]. Banovic D, Khorramshahi O, Owald D, Wichmann C, Riedt T, Fouquet W, Tian R, Sigrist SJ, Aberle H, Drosophila Neuroligin 1 promotes growth and postsynaptic differentiation at glutamatergic neuromuscular junctions, Neuron 66 (5) (2010) 724–738, doi:10.1016/j.neuron.2010.05.020. [PubMed: 20547130]

[3]. Barker JM, Bryant KG, Osborne JI, Chandler LJ, Age and sex interact to mediate the effects of intermittent, high-dose ethanol exposure on behavioral flexibility, Front. Pharmacol 8 (2017) 450, doi:10.3389/fphar.2017.00450. [PubMed: 28736526]

[4]. Berry A, Mazzelli M, Musillo C, Riva MA, Cattaneo A, Cirulli F, High-fat diet during adulthood interacts with prenatal stress, affecting both brain inflammatory and neuroendocrine markers in male rats, Eur. J. Neurosci 55 (9-10) (2022) 2326–2340, doi:10.1111/ejn.15181. [PubMed: 33711185]

[5]. Calabro FJ, Murty VP, Jalbrzikowski M, Tervo-Clemmens B, Luna B, Development of hippocampal-prefrontal cortex interactions through adolescence, Cereb. Cortex 30 (3) (2020) 1548–1558, doi:10.1093/cercor/bhz186. [PubMed: 31670797]

[6]. Cauley M, Hall BJ, Abreu-Villaca Y, Junaid S, White H, Kiany A, Slotkin TA, Levin ED, Critical developmental periods for effects of low-level tobacco smoke exposure on behavioral performance, Neurotoxicology 68 (2018) 81–87, doi:10.1016/j.neuro.2018.07.012. [PubMed: 30036564]

[7]. Centanni SW, Teppen T, Risher ML, Fleming RL, Moss JL, Acheson SK, Mulholland PJ, Pandey SC, Chandler LJ, Swartzwelder HS, Adolescent alcohol exposure alters GABAA receptor subunit expression in adult hippocampus, Alcohol Clin. Exp. Res 38 (11) (2014) 2800–2808, doi:10.1111/acer.12562. [PubMed: 25421517]

[8]. Chvatal A, Anderova M, Kirchhoff F, Three-dimensional confocal morphometry - a new approach for studying dynamic changes in cell morphology in brain slices, J. Anat 210 (6) (2007) 671–683, doi:10.1111/j.1469-7580.2007.00724.x. [PubMed: 17488344]

[9]. Crews FT, Robinson DL, Chandler LJ, Ehlers CL, Mulholland PJ, Pandey SC, Rodd ZA, Spear LP, Swartzwelder HS, Vetreno RP, Mechanisms of persistent neurobiological changes following adolescent alcohol exposure: NADIA consortium findings, Alcohol Clin. Exp. Res 43 (9) (2019) 1806–1822, doi:10.1111/acer.14154. [PubMed: 31335972]

[10]. Dawson DA, Goldstein RB, Chou SP, Ruan WJ, Grant BF, Age at first drink and the first incidence of adult-onset DSM-IV alcohol use disorders, Alcohol Clin. Exp. Res 32 (12) (2008) 2149–2160, doi:10.1111/j.1530-0277.2008.00806.x . [PubMed: 18828796]

[11]. Eichenbaum H, Prefrontal-hippocampal interactions in episodic memory, Nat. Rev. Neurosci 18 (9) (2017) 547–558, doi:10.1038/nrn.2017.74. [PubMed: 28655882]

[12]. Eroglu C, Allen NJ, Susman MW, O'Rourke NA, Park CY, Ozkan E, Chakraborty C, Mulinyawe SB, Annis DS, Huberman AD, Green EM, Lawler J, Dolmetsch R, Garcia KC, Smith SJ, Luo ZD, Rosenthal A, Mosher DF, Barres BA, Gabapentin receptor alpha2delta-1 is a neuronal thrombospondin receptor responsible for excitatory CNS synaptogenesis, Cell 139 (2) (2009) 380–392, doi:10.1016/j.cell.2009.09.025. [PubMed: 19818485]

[13]. Galaj E, Kipp BT, Floresco SB, Savage LM, Persistent alterations of accumbal cholinergic interneurons and cognitive dysfunction after adolescent intermittent ethanol exposure, Neuroscience 404 (2019) 153–164, doi:10.1016/j.neuroscience.2019.01.062. [PubMed: 30742967]

[14]. Garcia-Segura LM, Suarez I, Segovia S, Tranque PA, Calés JM, Aguilera P, Olmos G, Guillamón A, The distribution of glial fibrillary acidic protein in the adult rat brain is influenced by the neonatal levels of sex steroids, Brain Res. 456 (2) (1988) 357–363, doi:10.1016/0006-8993(88)90239-9. [PubMed: 3061565]

[15]. Gerraty RT, Davidow JY, Wimmer GE, Kahn I, Shohamy D, Transfer of learning relates to intrinsic connectivity between hippocampus, ventromedial prefrontal cortex, and large-scale networks, J. Neurosci 34 (34) (2014) 11297–11303, doi:10.1523/JNEUROSCI.0185-14.2014. [PubMed: 25143610]

[16]. Hanson KL, Cummins K, Tapert SF, Brown SA, Changes in neuropsychological functioning over 10 years following adolescent substance abuse treatment, Psychol. Addict. Behav 25 (1) (2011) 127–142, doi:10.1037/a0022350. [PubMed: 21443308]

[17]. Hawkey AB, White H, Pippen E, Greengrove E, Rezvani AH, Murphy SK, Levin ED, Paternal nicotine exposure in rats produces long-lasting neurobehavioral effects in the offspring, Neurotoxicol. Teratol 74 (2019) 106808, doi:10.1016/j.ntt.2019.05.001. [PubMed: 31103693]

[18]. He K, Lee A, Song L, Kanold PO, Lee HK, AMPA receptor subunit GluR1 (GluA1) serine-845 site is involved in synaptic depression but not in spine shrinkage associated with chemical long-term depression, J. Neurophysiol 105 (4) (2011) 1897–1907, doi:10.1152/jn.00913.2010. [PubMed: 21307330]

[19]. Healey KL, Kibble S, Bell A, Hodges S, Swartzwelder HS, Effects of adolescent intermittent ethanol on hippocampal expression of glutamate homeostasis and astrocyte-neuronal tethering proteins in male and female rats, J. Neurosci. Res (2020), doi:10.1002/jnr.24758.

[20]. Healey KL, Kibble S, Hodges S, Reissner KJ, Testen A, Wills TA, Acheson SK, Siemsen BM, McFaddin JA, Scofield MD, Swartzwelder HS, Enduring alterations in hippocampal astrocytesynaptic proximity following adolescent alcohol exposure: reversal by gabapentin, Neural Regen. Res 15 (8) (2020) 1496–1501, doi:10.4103/1673-5374.274339. [PubMed: 31997814]

[21]. Hegyi Z, Oláh T, Kőszeghy Á, Piscitelli F, HollY K, Pál B, Csernoch L, Di Marzo V, Antal M, CB(1) receptor activation induces intracellular Ca(2+) mobilization and 2-arachidonoylglycerol release in rodent spinal cord astrocytes, Sci. Rep 8 (1) (2018) 10562, doi:10.1038/s41598-018-28763-6. [PubMed: 30002493]

[22]. Kim R, Healey KL, Sepulveda-Orengo MT, Reissner KJ, Astroglial correlates of neuropsychiatric disease: From astrocytopathy to astrogliosis, Prog. Neuropsychopharmacol. Biol. Psychiatry 87 (2018) 126–146 Pt A, doi:10.1016/j.pnpbp.2017.10.002. [PubMed: 28989099]

[23]. Koss WA, Sadowski RN, Sherrill LK, Gulley JM, Juraska JM, Effects of ethanol during adolescence on the number of neurons and glia in the medial prefrontal cortex and basolateral amygdala of adult male and female rats, Brain Res. 1466 (2012) 24–32, doi:10.1016/j.brainres.2012.05.023. [PubMed: 22627163]

[24]. Lees B, Mewton L, Stapinski LA, Squeglia LM, Rae CD, Teesson M, Neurobiological and cognitive profile of young binge drinkers: a systematic review and meta-analysis, Neuropsychol. Rev 29 (3) (2019) 357–385, doi:10.1007/s11065-019-09411-w. [PubMed: 31512192]

[25]. Macht V, Elchert N, Crews F, Adolescent alcohol exposure produces protracted cognitive-behavioral impairments in adult male and female rats, Brain Sci. (11) (2020) 10, doi:10.3390/brainsci10110785. [PubMed: 33374858]

[26]. Mota N, Parada M, Crego A, Doallo S, Caamano-Isorna F, Rodriguez Holguin S, Cadaveira F, Corral M, Binge drinking trajectory and neuropsychological functioning among university students: a longitudinal study, Drug Alcohol Depend. 133 (1) (2013) 108–114 Epub 2013 Jun 19, doi:10.1016/j.drugalcdep.2013.05.024. [PubMed: 23791027]

[27]. Nguyen-Louie TT, Castro N, Matt GE, Squeglia LM, Brumback T, Tapert SF, Effects of emerging alcohol and marijuana use behaviors on adolescents' neuropsychological functioning over four years, J. Stud. Alcohol Drugs 76 (5) (2015) 738–748 https://www.ncbi.nlm.nih.gov/pubmed/26402354. [PubMed: 26402354]

[28]. Nguyen-Louie TT, Tracas A, Squeglia LM, Matt GE, Eberson-Shumate S, Tapert SF, Learning and memory in adolescent moderate, binge, and extreme-binge drinkers, Alcohol Clin. Exp. Res 40 (9) (2016) 1895–1904 Epub 2016 Jul 27, doi:10.1111/acer.13160. [PubMed: 27462830]

[29]. Oberheim NA, Goldman SA, Nedergaard M, Heterogeneity of astrocytic form and function, Methods Mol. Biol 814 (2012) 23–45, doi:10.1007/978-1-61779-452-0_3 . [PubMed: 22144298]

[30]. Patel R, Dickenson AH, Mechanisms of the gabapentinoids and α 2 δ-1 calcium channel subunit in neuropathic pain, Pharmacol. Res. Perspectives 4 (2) (2016) e00205–e00205, doi:10.1002/prp2.205.

[31]. Paxinos G, Watson C, The Rat Brain In Stereotaxic Coordinates, Academic Press, 1982.

[32]. Pekny M, Pekna M, Messing A, Steinhauser C, Lee JM, Parpura V, Hol EM, Sofroniew MV, Verkhratsky A, Astrocytes: a central element in neurological diseases, Acta Neuropathol. 131 (3) (2016) 323–345 Epub 2015 Dec 15, doi:10.1007/s00401-015-1513-1 . [PubMed: 26671410]

[33]. Pfau DR, Hobbs NJ, Breedlove SM, Jordan CL, Sex and laterality differences in medial amygdala neurons and astrocytes of adult mice, J. Comp. Neurol 524 (12) (2016) 2492–2502, doi:10.1002/cne.23964. [PubMed: 26780286]

[34]. Qu Y, Galvan A, Fuligni AJ, Lieberman MD, Telzer EH, Longitudinal changes in prefrontal cortex activation underlie declines in adolescent risk taking, J. Neurosci 35 (32) (2015) 11308–11314, doi:10.1523/JNEUROSCI.1553-15.2015. [PubMed: 26269638]

[35]. Rajkowska G, Stockmeier CA, Astrocyte pathology in major depressive disorder: insights from human postmortem brain tissue, Curr. Drug Targets 14 (11) (2013) 1225–1236 https://www.ncbi.nlm.nih.gov/pubmed/23469922. [PubMed: 23469922]

[36]. Ribeiro-Carvalho A, Lima CS, Dutra-Tavares AC, Nunes F, Nunes-Freitas AL, Filgueiras CC, Manhaes AC, Meyer A, Abreu-Villaca Y, Mood-related behavioral and neurochemical alterations in mice exposed to low chlorpyrifos levels during the brain growth spurt, PLoS One 15 (10) (2020) e0239017, doi:10.1371/jour-nal.pone.0239017. [PubMed: 33007016]

[37]. Ridderinkhof KR, Ullsperger M, Crone EA, Nieuwenhuis S, The role of the medial frontal cortex in cognitive control, Science 306 (5695) (2004) 443–447, doi: 10.1126/science.1100301. [PubMed: 15486290]

[38]. Risher ML, Fleming RL, Risher WC, Miller KM, Klein RC, Wills T, Acheson SK, Moore SD, Wilson WA, Eroglu C, Swartzwelder HS, Adolescent intermittent alcohol exposure: persistence of structural and functional hippocampal abnormalities into adulthood, Alcohol Clin. Exp. Res 39 (6) (2015) 989–997 Epub 2015 Apr 27, doi:10.1111/acer.12725. [PubMed: 25916839]

[39]. Risher ML, Sexton HG, Risher WC, Wilson WA, Fleming RL, Madison RD, Moore SD, Eroglu C, Swartzwelder HS, Adolescent intermittent alcohol exposure: dysregulation of thrombospondins and synapse formation are associated with decreased neuronal density in the adult hippocampus, Alcohol Clin. Exp. Res 39 (12) (2015) 2403–2413 Epub 2015 Nov 5, doi:10.1111/acer.12913. [PubMed: 26537975]

[40]. Schätzle P, Wuttke R, Ziegler U, Sonderegger P, Automated quantification of synapses by fluorescence microscopy, J. Neurosci. Methods 204 (1) (2012) 144–149, doi:10.1016/j.jneumeth.2011.11.010. [PubMed: 22108140]

[41]. Scofield MD, Li H, Siemsen BM, Healey KL, Tran PK, Woronoff N, Boger HA, Kalivas PW, Reissner KJ, Cocaine self-administration and extinction leads to reduced glial fibrillary acidic protein expression and morphometric features of astrocytes in the nucleus accumbens core, Biol. Psychiatry 80 (3) (2016) 207–215 Epub 2015 Dec 31, doi:10.1016/j.biopsych.2015.12.022. [PubMed: 26946381]

[42]. Siemsen BM, Giannotti G, McFaddin JA, Scofield MD, McGinty JF, Biphasic effect of abstinence duration following cocaine self-administration on spine morphology and plasticity-related proteins in prelimbic cortical neurons projecting to the nucleus accumbens core, Brain Struct. Funct 224 (2) (2019) 741–758, doi:10.1007/s00429-018-1805-z. [PubMed: 30498893]

[43]. Siemsen BM, Reichel CM, Leong KC, Garcia-Keller C, Gipson CD, Spencer S, McFaddin JA, Hooker KN, Kalivas PW, Scofield MD, Effects of methamphetamine self-administration and extinction on astrocyte structure and function in the nucleus accumbens core, Neuroscience 406 (2019) 528–541, doi:10.1016/j.neuroscience.2019.03.040. [PubMed: 30926546]

[44]. Snedecor GW, Cochran WG, Statistical methods, 7th ed., Iowa State University Press, 1980.

[45]. Spear LP, The adolescent brain and age-related behavioral manifestations, Neurosci. Biobehav. Rev 24 (4) (2000) 417–463 https://www.ncbi.nlm.nih.gov/pubmed/10817843. [PubMed: 10817843]

[46]. Spear LP, Effects of adolescent alcohol consumption on the brain and behaviour, Nat. Rev. Neurosci 19 (2018) 197, doi:10.1038/nrn.2018.10. [PubMed: 29467469]

[47]. Spear LP, Swartzwelder HS, Adolescent alcohol exposure and persistence of adolescent-typical phenotypes into adulthood: a mini-review, Neurosci. Biobehav. Rev 45 (2014) 1–8 Epub 2014 May 9, doi:10.1016/j.neubiorev.2014.04.012. [PubMed: 24813805]

[48]. Squeglia LM, Tapert SF, Sullivan EV, Jacobus J, Meloy MJ, Rohlfing T, Pfefferbaum A, Brain development in heavy-drinking adolescents, Am. J. Psychiatry 172 (6) (2015) 531–542, doi:10.1176/appi.ajp.2015.14101249. [PubMed: 25982660]

[49]. Suto T, Severino AL, Eisenach JC, Hayashida K.-i., Gabapentin increases extracellular glutamatergic level in the locus coeruleus via astroglial glutamate transporter-dependent mechanisms, Neuropharmacology 81 (2014) 95–100, doi:10.1016/j.neuropharm.2014.01.040. [PubMed: 24495399]

[50]. Swartzwelder HS, Healey KL, Liu W, Dubester K, Miller KM, Crews FT, Changes in neuroimmune and neuronal death markers after adolescent alcohol exposure in rats are reversed by donepezil, Sci. Rep 9 (1) (2019) 12110, doi:10.1038/s41598-019-47039-1. [PubMed: 31431637]

[51]. Swartzwelder HS, Park MH, Acheson S, Adolescent ethanol exposure enhances NMDA receptor-mediated currents in hippocampal neurons: reversal by gabapentin, Sci. Rep 7 (1) (2017) 13133, doi:10.1038/s41598-017-12956-6. [PubMed: 29030575]

[52]. Taylor CP, Harris EW, Analgesia with gabapentin and pregabalin may involve n-methyl-d-aspartate receptors, neurexins, and thrombospondins, J. Pharmacol. Exp. Ther 374 (1) (2020) 161–174, doi:10.1124/jpet.120.266056. [PubMed: 32321743]

[53]. Testen A, Ali M, Sexton HG, Hodges S, Dubester K, Reissner KJ, Swartzwelder HS, Risher ML, Region-specific differences in morphometric features and synaptic colocalization of astrocytes during development, Neuroscience 400 (2019) 98–109 Epub 2018 Dec 29, doi:10.1016/j.neuroscience.2018.12.044. [PubMed: 30599266]

[54]. Testen A, Sepulveda-Orengo MT, Gaines CH, Reissner KJ, Region-specific reductions in morphometric properties and synaptic colocalization of astrocytes following cocaine self-administration and extinction, Front. Cell Neurosci 12 (2018) 246, doi:10.3389/fncel.2018.00246. [PubMed: 30147645]

[55]. Towner TT, Spear LP, Rats exposed to intermittent ethanol during late adolescence exhibit enhanced habitual behavior following reward devaluation, Alcohol 91 (2021) 11–20, doi:10.1016/j.alcohol.2020.09.004. [PubMed: 33031883]

[56]. Trantham-Davidson H, Centanni SW, Garr SC, New NN, Mulholland PJ, Gass JT, Glover EJ, Floresco SB, Crews FT, Krishnan HR, Pandey SC, Chandler LJ, Binge-like alcohol exposure during adolescence disrupts dopaminergic neurotransmission in the adult prelimbic cortex, Neuropsychopharmacology 42 (5) (2017) 1024–1036 Epub 2016 Sep 13, doi:10.1038/npp.2016.190. [PubMed: 27620551]

[57]. Varlinskaya EI, Hosová D, Towner T, Werner DF, Spear LP, Effects of chronic intermittent ethanol exposure during early and late adolescence on anxiety-like behaviors and behavioral flexibility in adulthood, Behav. Brain Res 378 (2020) 112292, doi:10.1016/j.bbr.2019.112292. [PubMed: 31626849]

[58]. Verkhratsky A, Rodriguez JJ, Steardo L, Astrogliopathology: a central element of neuropsychiatric diseases? Neuroscientist 20 (6) (2014) 576–588, doi:10.1177/1073858413510208. [PubMed: 24301046]

[59]. Viner RM, Taylor B, Adult outcomes of binge drinking in adolescence: findings from a UK national birth cohort, J. Epidemiol. Community Health 61 (10) (2007) 902–907, doi:10.1136/jech.2005.038117. [PubMed: 17873228]

[60]. Walter TJ, Vetreno RP, Crews FT, Alcohol and stress activation of microglia and neurons: brain regional effects, Alcohol Clin. Exp. Res 41 (12) (2017) 2066–2081, doi: 10.1111/acer.13511. [PubMed: 28941277]

[61]. White AM, Kraus CL, Swartzwelder H, Many college freshmen drink at levels far beyond the binge threshold, Alcohol Clin. Exp. Res 30 (6) (2006) 1006–1010, doi:10.1111/j.1530-0277.2006.00122.x. [PubMed: 16737459]

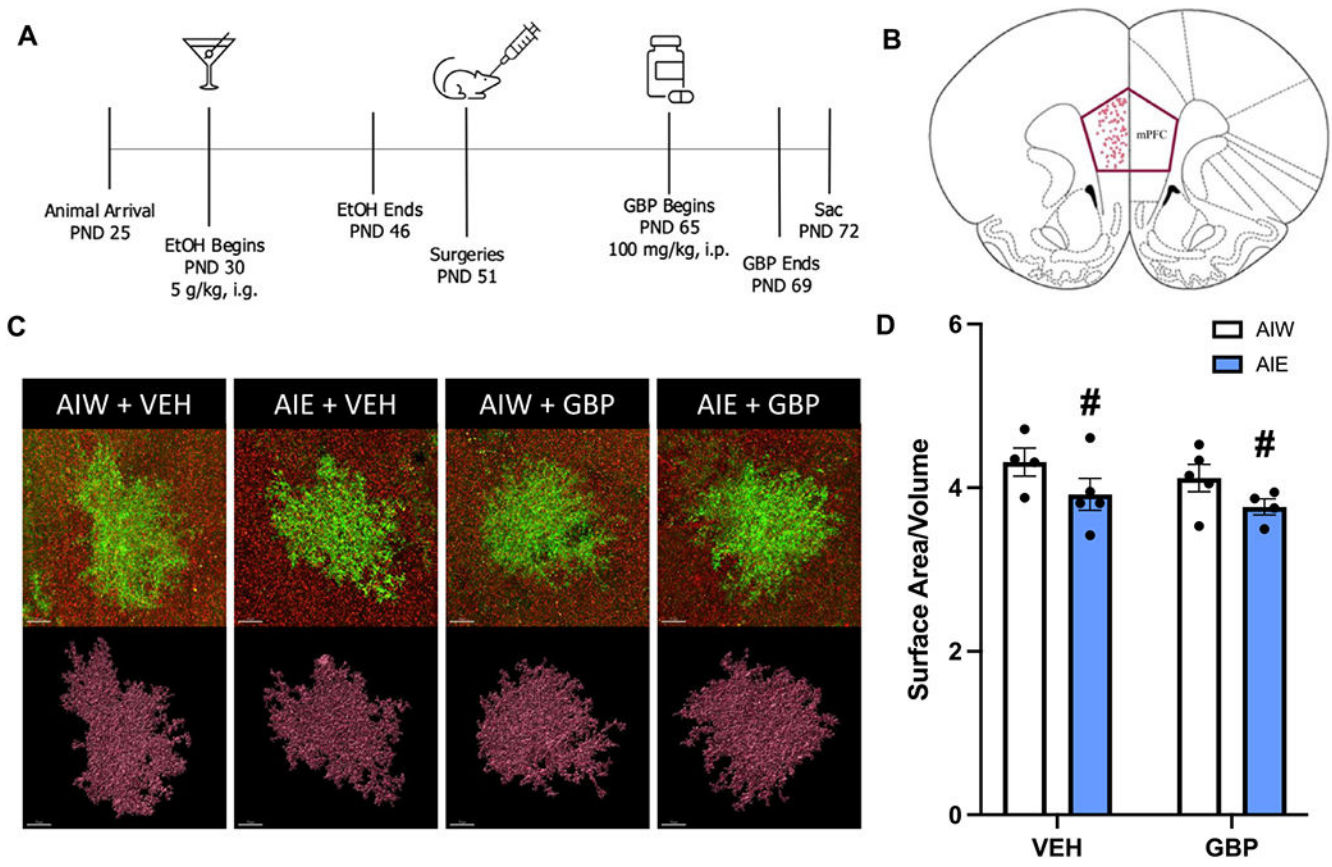

Fig. 1. AIE + Gabapentin significantly reduced astrocyte surface area to volume.

(A) Experimental Timeline. AIW = Adolescent Intermittent Water (i.g), AIE = Adolescent Intermittent Ethanol (5 g/kg, i.g.), VEH = vehicle (0.9% sterile saline, i.p.), GBP = gabapentin (100 mg/kg, i.p.). There are four treatment groups: AIW + VEH (n = 4), AIE + VEH (n = 5), AIW + GBP (n = 5), AIE + GBP (n = 4). The number of analyzed astrocytes are as follows: AIW + VEH (n = 19), AIE + VEH (n = 20), AIW + GBP (n = 17), AIE + GBP (n = 17). **(B)** Pink dots represent the locations of the 73 astrocytes imaged in the mPFC. Illustration from Paxinos & Watson (1997). **(C)** The signal of the LCK-GFP virus (green) and the signal of the GluA1 marked synaptic puncta (red) are both strong and clear so that both the surface of the astrocyte and the colocalized synaptic puncta can be synthesized. Columns – Treatment groups. Row 1 – Raw z-series of a single slice astrocyte (green) and GluA1 synaptic puncta (red). Row 2 - Rendered 3-D structure of astrocyte (pink) using surface function of Imaris software. Scale bars are 10 μm. **(D)** Mean (± SEM) ratio of astrocyte surface area to volume was significantly reduced by the exposure to AIE ($F_{(1,14)} = 4.87$, $p = 0.04$). "#" represents main effect. Dots represent individual astrocytes while bars represent data from averaged animals.

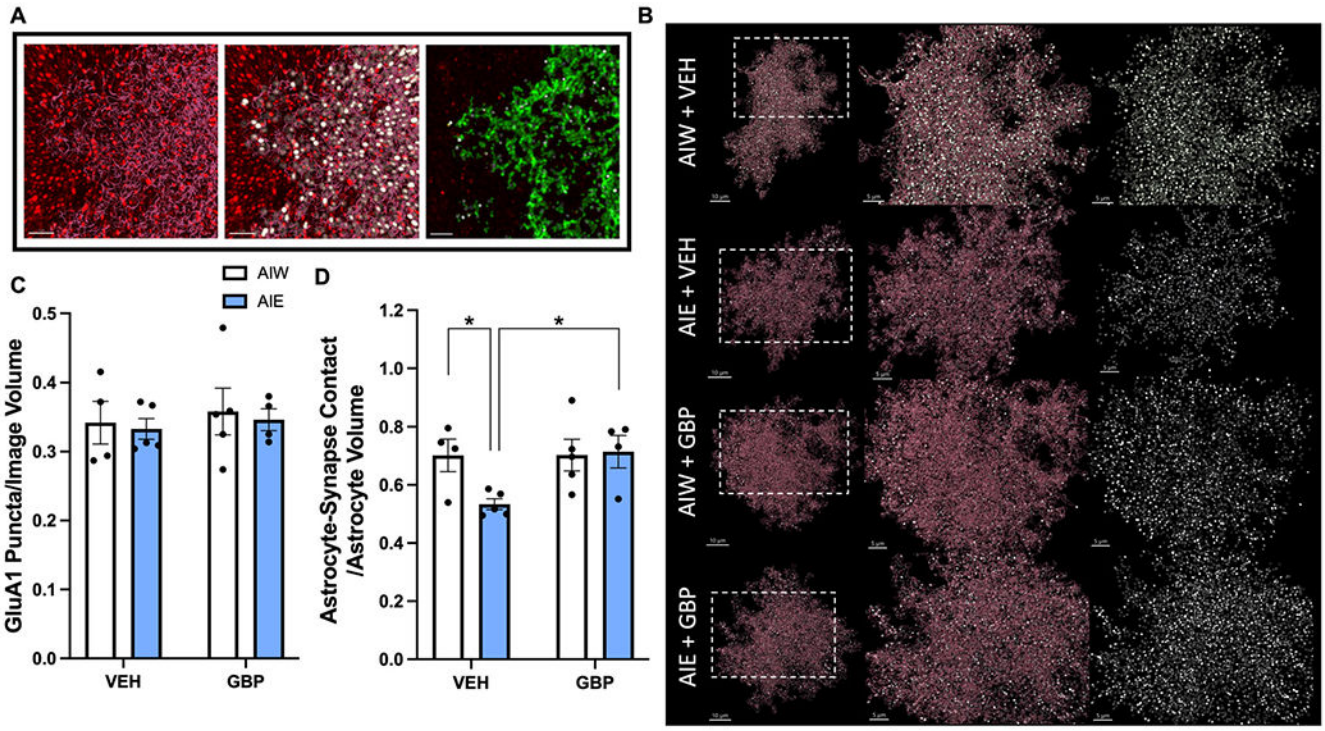

Fig. 2. AIE-induced reduction of astrocyte-synaptic proximity is reversed by gabapentin.

(A) Representation of colocalization methods. Left panel - rendered astrocyte surface outline (pink) and raw GluA1 puncta (red), Middle panel – GluA1 puncta (red) and a subset that are in contact (white) with astrocyte membrane (pink) (Astrocyte-Synaptic Contact). Right panel – raw z-slice of astrocyte (green) and Astrocyte-Synaptic Contact (white), GluA1 puncta (red, not colocalized with astrocyte). **(B)** Rows – Treatment groups: AIW = Adolescent Intermittent Water (i.g), AIE = Adolescent Intermittent Ethanol (5 g/kg, i.g.), VEH = vehicle (0.9% sterile saline, i.p.), GBP = gabapentin (100 mg/kg, i.p.). Column 1 - Rendered surface of astrocyte (pink) with colocalized synaptic puncta (white). Scale bars are 10 μm. Column 2 – Expanded magnification of inset box in Column 1. Scale bars are 5 μm. Column 3 – Expanded magnification of colocalized synaptic puncta (white). Scale bars are 5 μm. The ROI colocalized density (white) is significantly reduced in AIE exposed animals who were not treated with gabapentin compared to all other treatment groups. **(C)** Mean (± SEM) density of GluA1 synaptic puncta was unchanged by AIE exposure or gabapentin treatment ($p > 0.05$). **(D)** Mean (± SEM) ROI colocalization density was significantly reduced in animals exposed to AIE compared to AIW control animals ($p < 0.05$), and this effect was reversed by gabapentin (AIE + GBP vs. AIE, $p < 0.05$; AIE + GBP vs. AIW + GBP, $p > 0.05$). "*" represents simple main effect. Dots represent individual astrocytes while bars represent data from averaged animals.

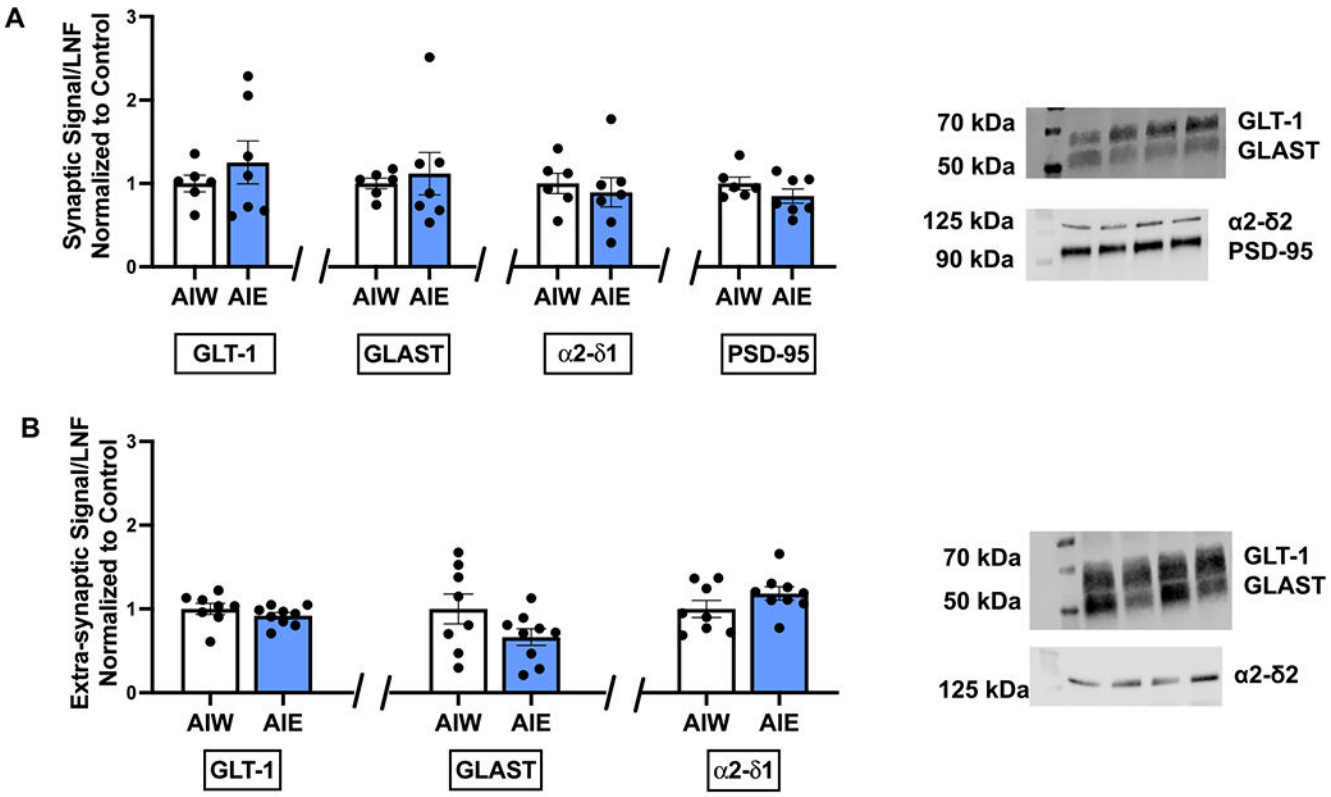

Fig. 3. No significant effect of either AIE on protein expression of GLT-1, GLAST, α2-δ1 or PSD-95.

(A) Mean (± SEM) protein expression of GLT-1, GLAST, α2-δ1, and PSD-95 was unchanged by AIE treatment (blue) in the synaptic fractionation. **(B)** Mean (± SEM) protein expression of GLT-1, GLAST, and α2-δ1 was unchanged by AIE treatment (blue) in the extra-synaptic fractionation. Images on the right include representative bands for each protein to demonstrate sufficient expression for analysis. See supplemental Figs. for full images of PVDF membranes with protein expression. AIW = Adolescent Intermittent Water (i.g), AIE = Adolescent Intermittent Ethanol (5 g/kg, i.g.).